Spring greening induced autumnal runoff reduction across the high latitudes

Extended Data Figure 1. Spatial and temporal changes of Seasonal vegetation growth (leaf area index, LAI and normalized difference vegetation index, NDVI) during 1982-2020. (a-c) Spatial temporal changes of (a) Spring LAI, (b) Summer LAI and (c) Autumn LAI. (d-f) Spatial temporal changes of (d) Spring NDVI, (e) Summer NDVI and (f) Autumn NDVI. The bottom left subgraph represents the data distribution, the dash lines represent mean values, and the regions marked by slashes indicate significant changes.

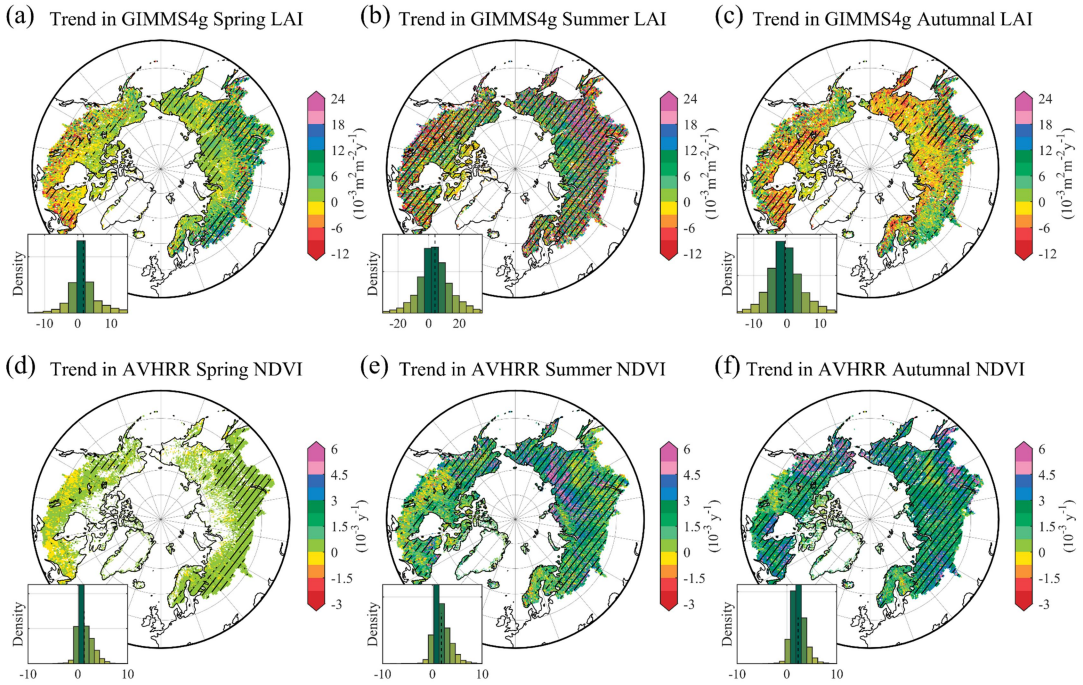

Extended Data Figure 2. The change trend of monthly leaf area index (LAI) during 1982-2014. The lower left subgraph represents the frequency distribution of the trends. The regions marked by slashes indicate significant changes. The notation above each sub-graph is the abbreviation of the month (January to December).

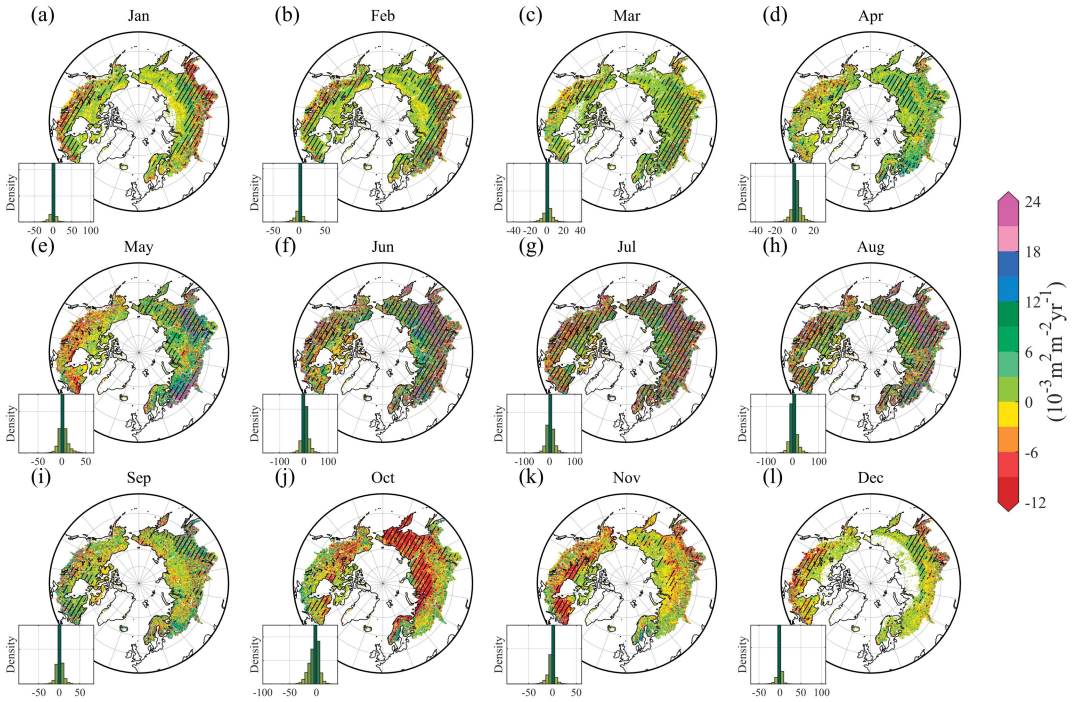

Extended Data Figure 3. Spatial distribution and seasonal variations of monthly mean burned area from 1982 to 2014. The panels (a-l) display the multi-year average of burned area (km^2) for each month, from January to December, respectively. The color scale indicates the magnitude of the burned area, with darker red representing higher fire activity. The notation above each sub-graph is the abbreviation of the month (January to December).

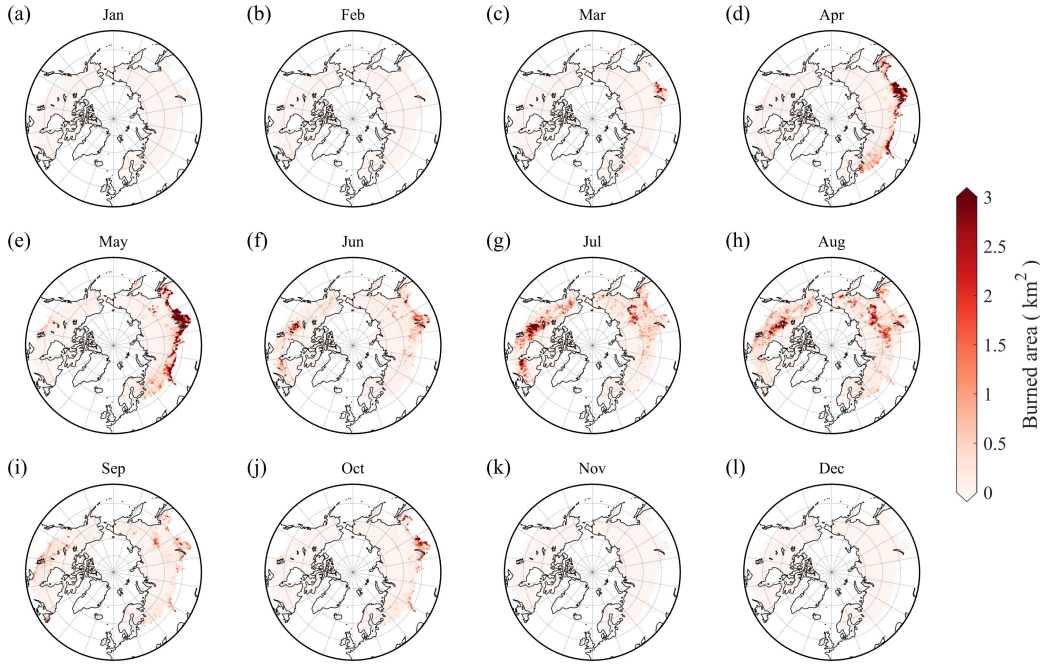

Extended Data Figure 4. Relationship between vegetation greening trends and burned area in Northern America. Bivariate kernel density plots and marginal distributions of Leaf Area Index (LAI) trends (m^2m^{-2} y^{-1}) versus burned area (km^2) during spring and summer across Northern America (45.25 ° N-70.25 ° N, 179.75 ° W-55.25 ° W). The x-axis is presented on a logarithmic scale (log10) to account for the wide range of fire magnitudes. Shaded areas in the main panel represent the estimated probabilistic density of data points, with darker colors indicating higher data concentration. Solid lines denote the linear regression fits between LAI trends and log10-transformed burned area. Regression equations and associated P-values (calculated via F-test) are shown in the upper-left corner, indicating the statistical significance of the cross-seasonal relationships. Top and right panels display the marginal kernel density estimates for burned area and LAI trends, respectively.

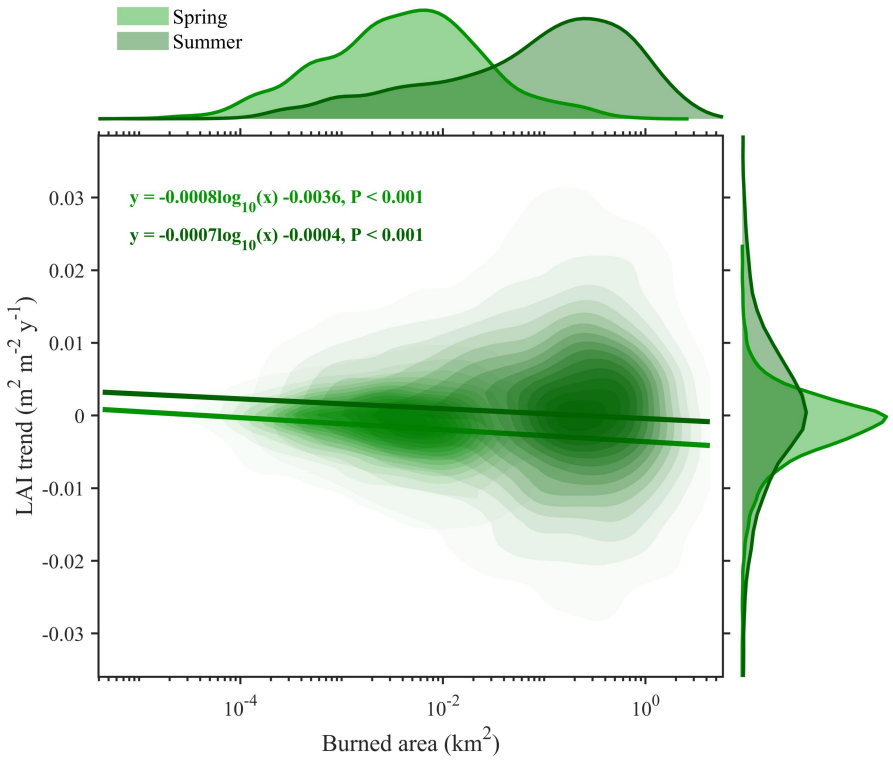

Extended Data Figure 5. Spatial distribution of the change trend of observed autumn runoff during 1982-2014. Each basin is colored according to the magnitude of the variation trend. The upper right subchart counts the number of stations-years in the observed watershed.

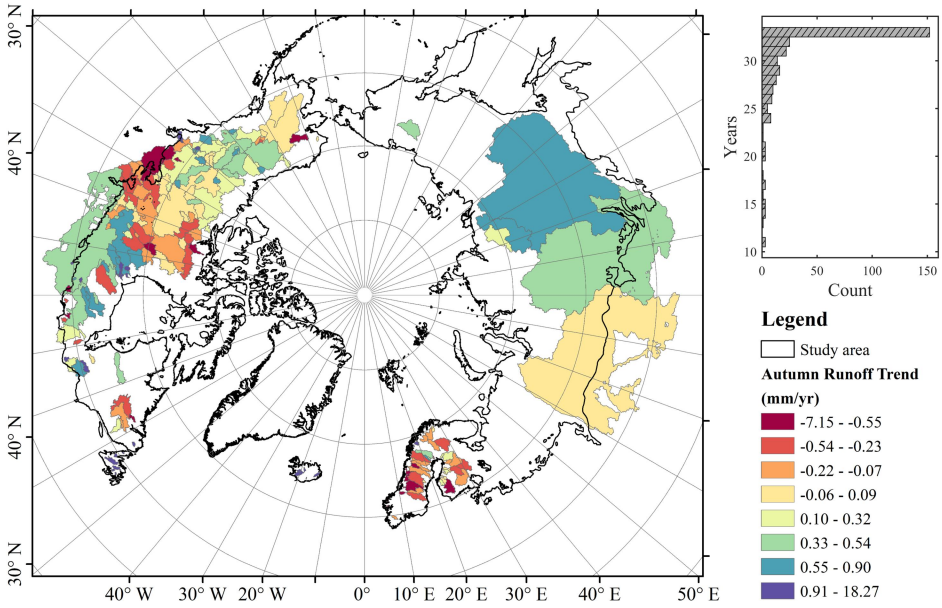

Extended Data Figure 6. The change trend of precipitation minus Runoff (P-Q) deficit during 1982-2014. (a) Spatial distribution of the change trend, P: precipitation and Q: runoff. The black dots represent areas of significant change. (b) Frequency distribution of that trend among different plant functional types.

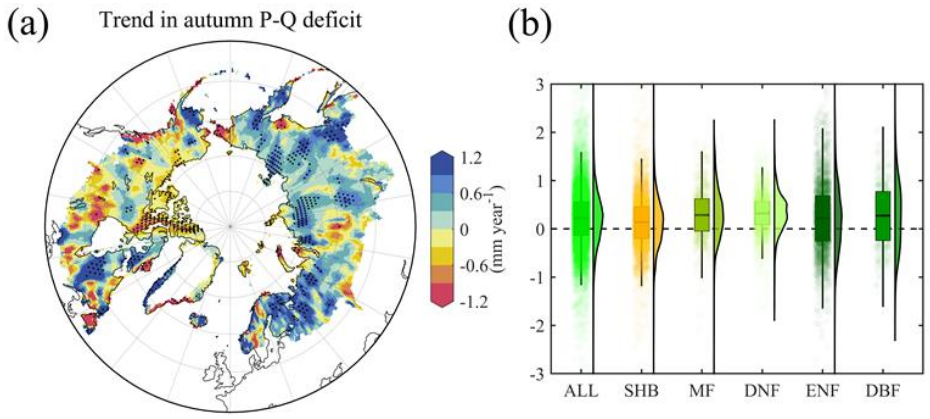

Extended Data Figure 7. The spatial distribution of landcover types in the GLC2000 products and study area of this research. The black polygon represents the tundra and boreal regions.

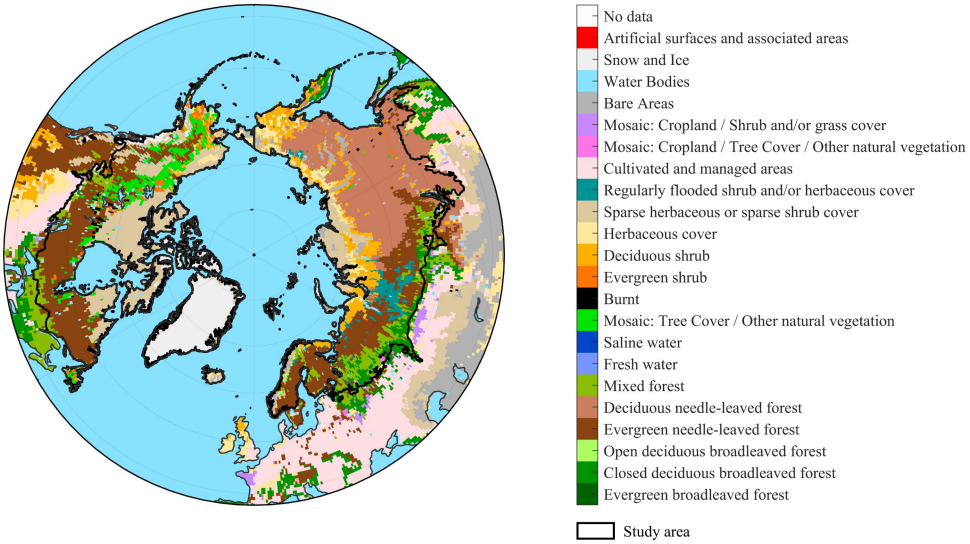

Extended Data Figure 8. The joint distribution of seasonal vegetation growth (LAI, $m^2m^{-2}year^{-1}$) and autumn runoff (mm $year^{-1}$) trends in where autumn precipitation remained nearly unchanged (<0.1 mm yr^{-1}). The greener the color, the higher the data density. The solid black lines represent linear fit between autumn runoff and vegetation growth in different seasons.

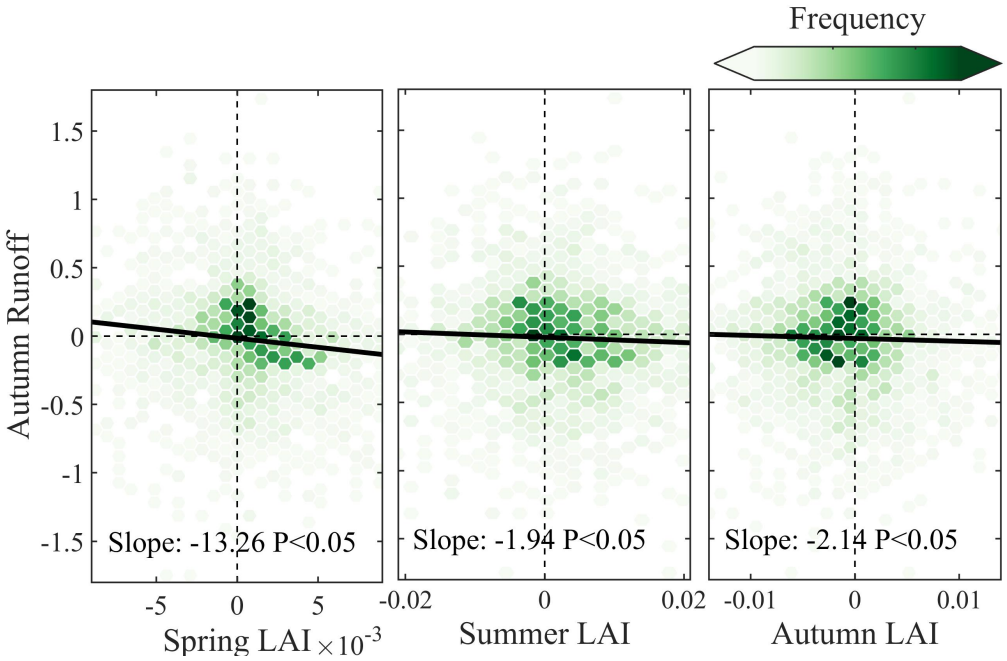

Extended Data Figure 9. The joint distribution of seasonal vegetation growth (NDVI, 10^{-3} year^{-1}) and autumn runoff (mm year^{-1}) trends in where autumn precipitation remained nearly unchanged (<0.1 mm yr^{-1}). The greener the color, the higher the data density. The solid black lines represent linear fit between autumn runoff and vegetation growth in different seasons.

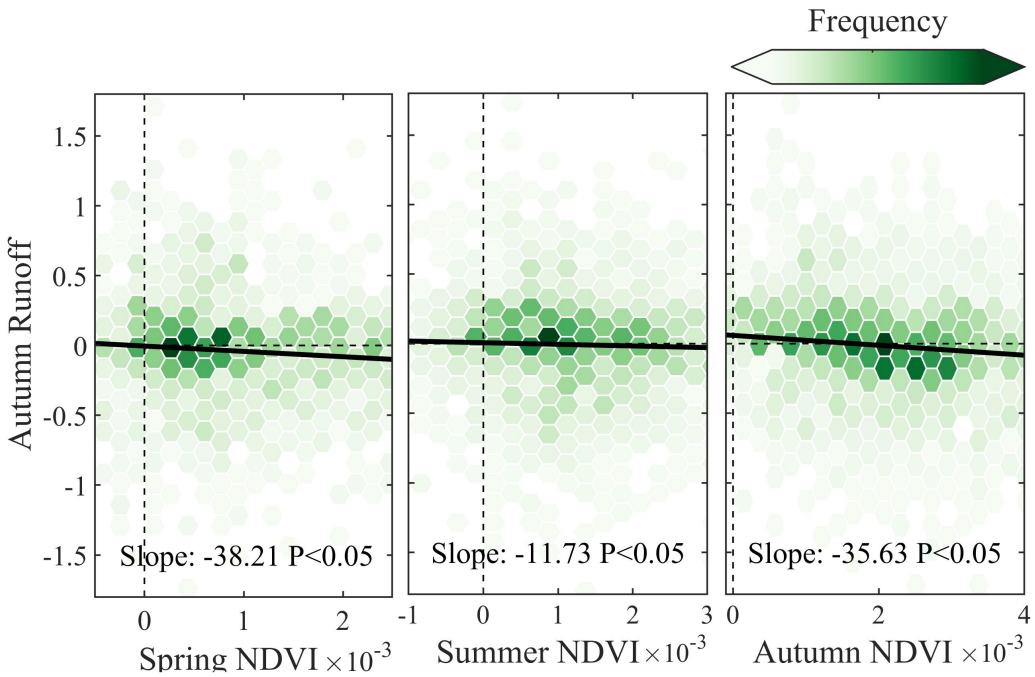

Extended Data Figure 10. The spatial pattern of vegetation phenological events and the months it belongs to. (a-c) Spatial pattern of (a) SOS, (b) POS and (c) EOS. (d-f) Spatial pattern of months that (d) SOS, (e) POS and (f) EOS belongs to. The bottom left subgraph represents the data distribution.

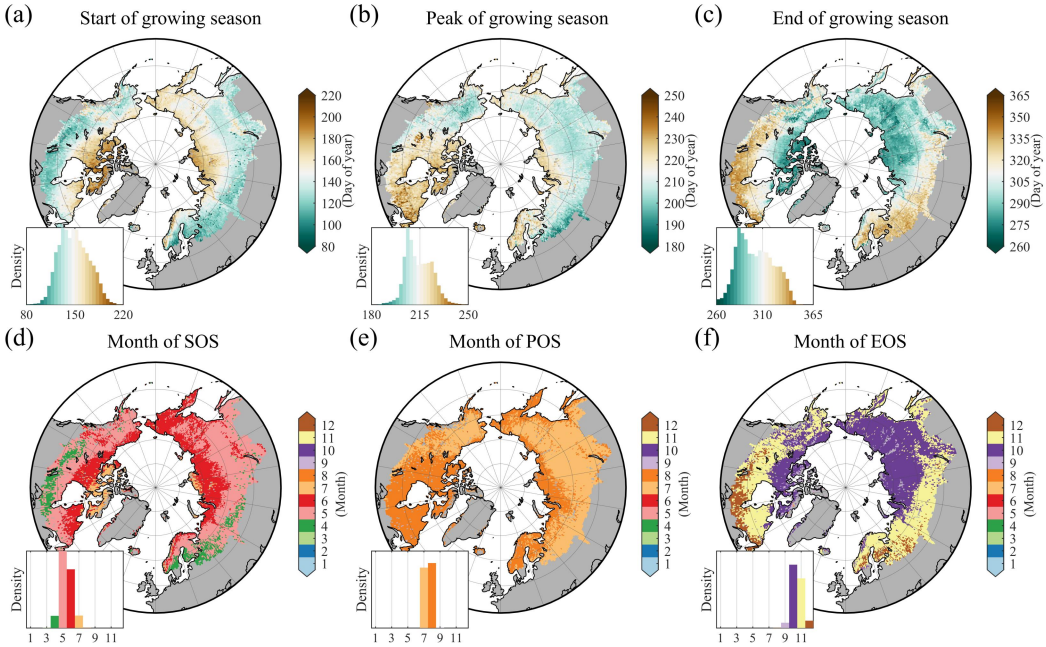

Extended Data Figure 11. Frequency distribution of phenological events, (a) EOS and (b) SOS, across different plant functional types during 1982-2014.

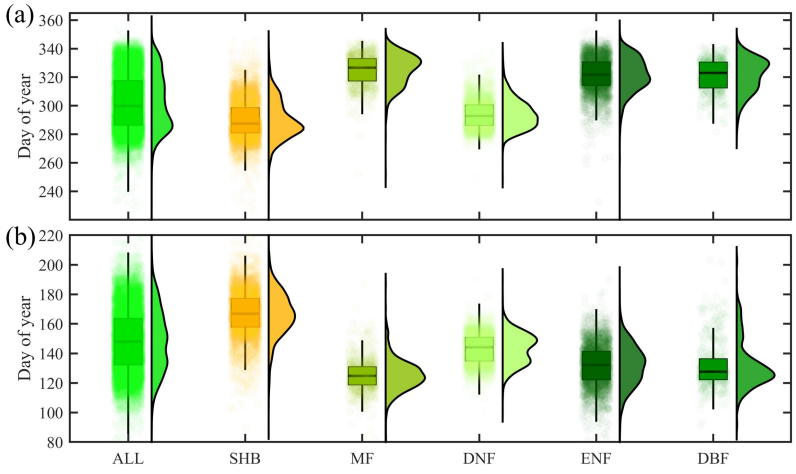

Extended Data Figure 12. Ridge regressions between seasonal vegetation growth and monthly autumnal runoff. (a-c) Spatial distributions of the ridge-regression coefficients (magnitudes and directions of the effects are denoted by the values; specifically, negative coefficients indicate that vegetation greening decreases autumnal monthly runoff) between spring NDVI and (a) September (Sep), (b) October (Oct) and (c) November (Nov) monthly runoff. (d) Kernel density estimates of the frequency distributions of ridge-regression coefficients across different plant functional types. (e-g) Same as (a-c) but for summer NDVI. (h) Same as (d) but for summer NDVI. The dashed lines represent means.

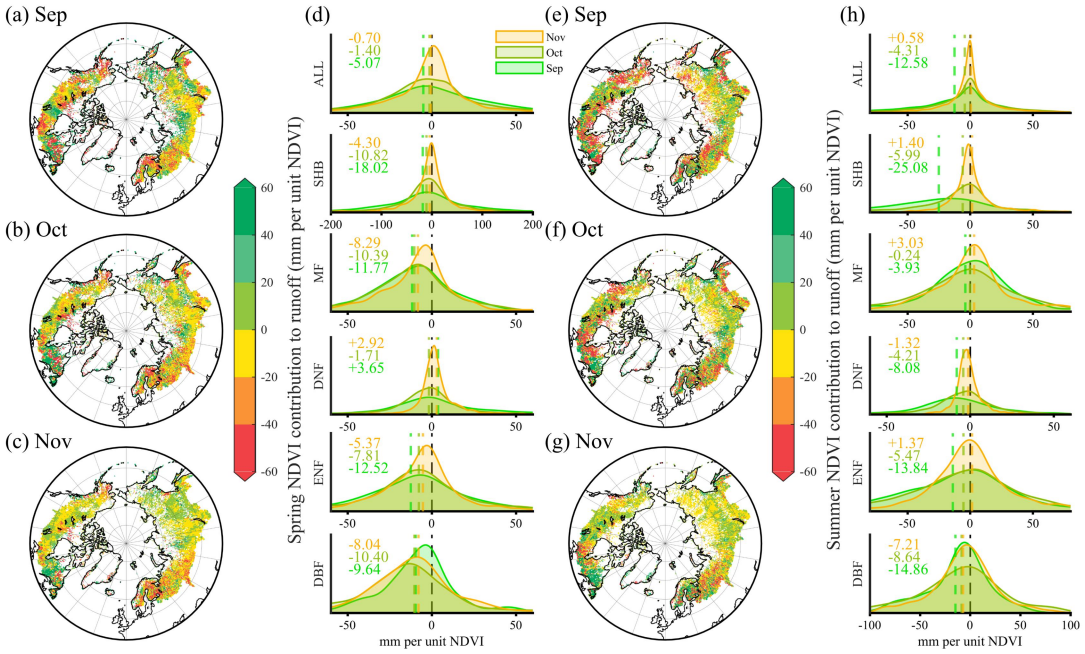

Extended Data Figure 13. LPJ-GUESS simulated autumn runoff variation trend (mm year^{-1}) during 1982-2014. (a) Spatial pattern of autumn runoff trends simulated by LPJ-GUESS. The lower left subgraph represents the frequency distribution of the trends. The black dots represent areas of significant change. (b) Grid-scale comparison of runoff trends between LPJ-GUESS and GRUN. Hexagonal bins represent density. The solid line denotes the linear fit (slope = 0.9, P < 0.05); dashed lines indicate zero trends.

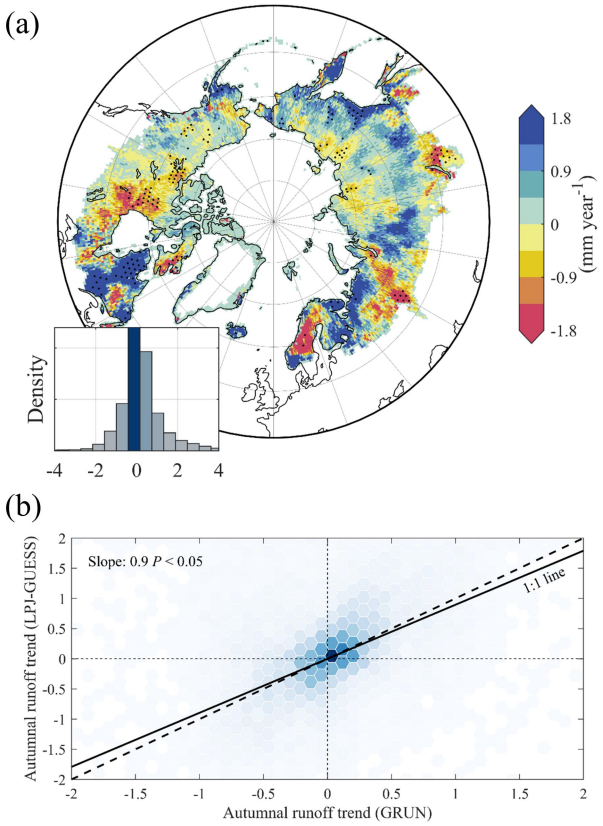

Extended Data Figure 14. Spring phenology (leaf onset) of a given grid cell simulated by LPJ-GUESS of two scenarios (Control vegetation minus Contrast). The gray shaded area indicates the period (1982–1986) used to calculate the meteorological forcing for the phenology module.

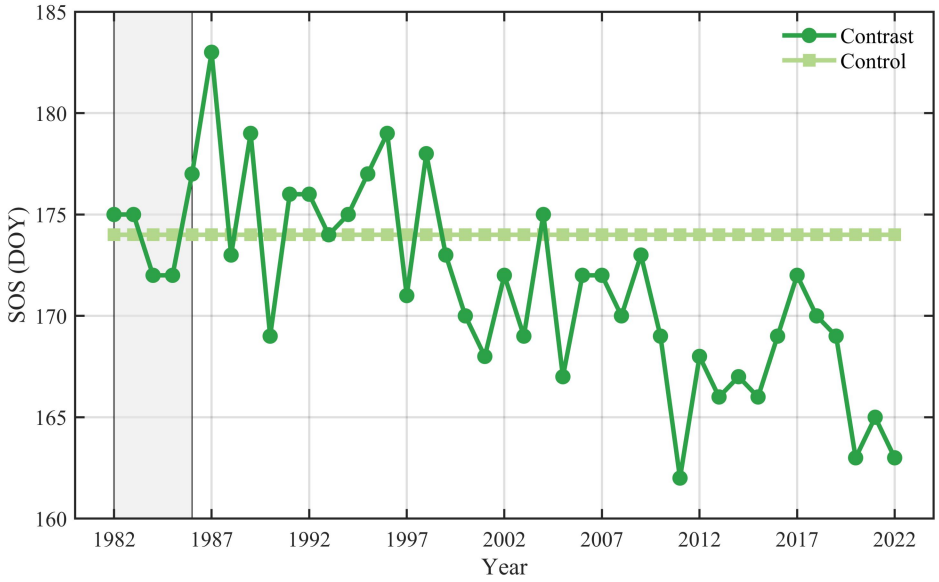

Extended Data Figure 15. The scatter plot between Delta leaf area index (spring and summer) and Delta autumn runoff simulated by LPJ-GUESS of two scenarios (Control vegetation minus Contrast). The darker the green, the higher the density of the dots. The solid black lines represent linear fit between delta autumn runoff and delta leaf area index (spring and summer).

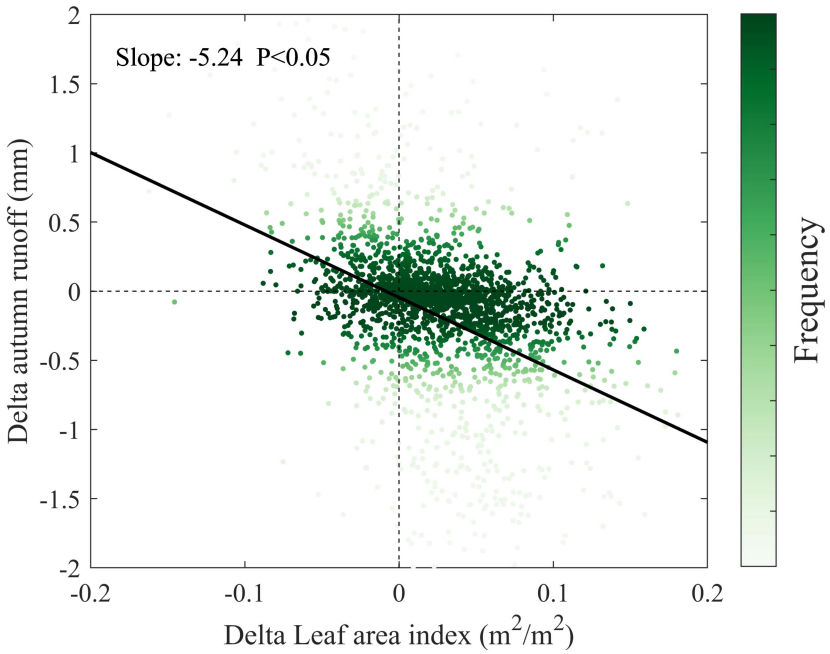

Extended Data Figure 16. LPJ-GUESS simulated variations in autumnal monthly runoff. (a-c) Spatial distributions of simulated runoff differences between the experimental and control runs for (a) September (Sep), (b) October (Oct), and (c) November (Nov). The color scale indicates the magnitude and direction of the simulated runoff changes (%), with positive values representing increased runoff and negative values indicating decreased runoff in the experimental simulations. (d) Kernel density estimates of the frequency distributions of runoff differences across various plant functional types (PFTs). Vertical dashed lines indicate the mean values for each month: September (green), October (light green), and November (orange).

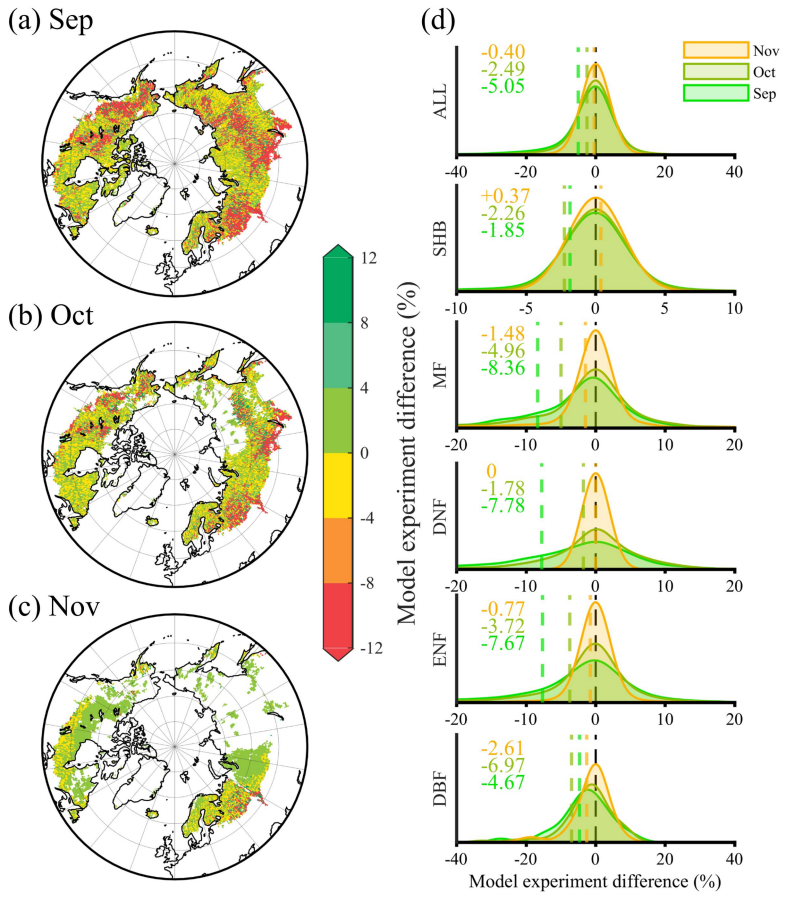

Extended Data Figure 17. Variation in growing season length (GSL) across vegetation types with differing cross-seasonal effect (CSE) persistence. Letters (a, b, c) indicate statistically significant differences between groups ($p < 0.05$, two-tailed unpaired t-test). SHB, shrub; MF, mixed forest; DNF, deciduous needle-leaved forest; ENF, evergreen needle-leaved forest; DBF, deciduous broadleaved forest.

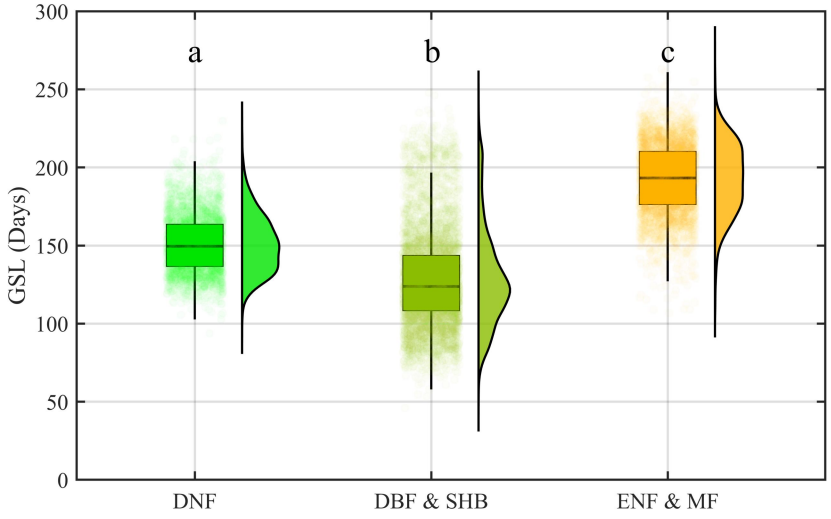

Extended Data Figure 18. LPJ-GUESS model simulated effects of seasonal vegetation growth on monthly runoff in autumn among different plant functional types during 1982-2022. The number in parentheses in the tick label on the Y-axis represents the number of grid points counted.

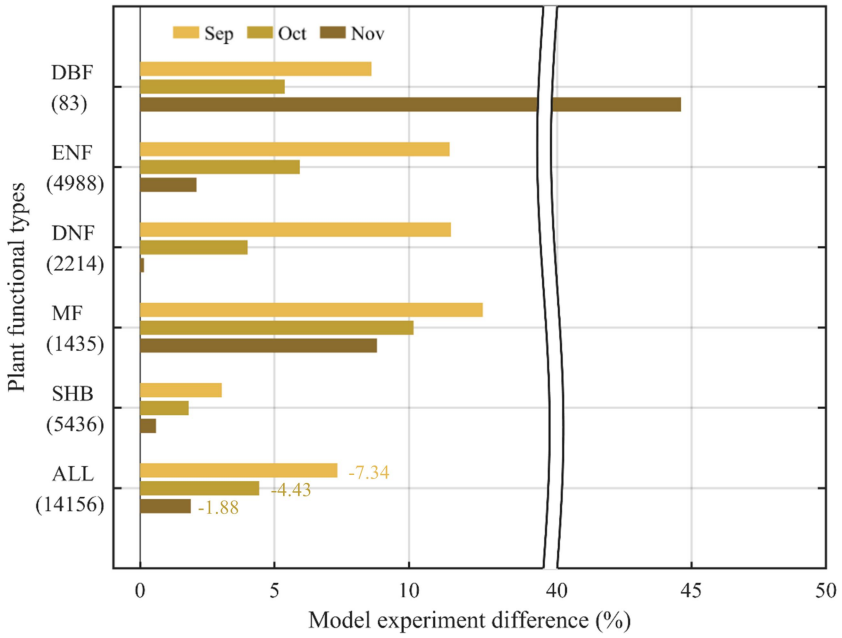

Extended Data Figure 19. Relationship among changes in leaf area index (LAI), summer soil water content (SWC), and autumn runoff derived from LPJ-GUESS scenario experiments (Control vegetation minus Contrast). Darker blue indicating higher point density. The grey plane shows the multiple linear regression surface, illustrating the joint effects of ΔLAI and ΔSWC on ΔRunoff. Black lines denote the zero-reference axes. Regression slopes and associated significance levels ($p < 0.05$) are indicated, highlighting the negative association between vegetation growth and autumn runoff mediated by soil moisture changes.

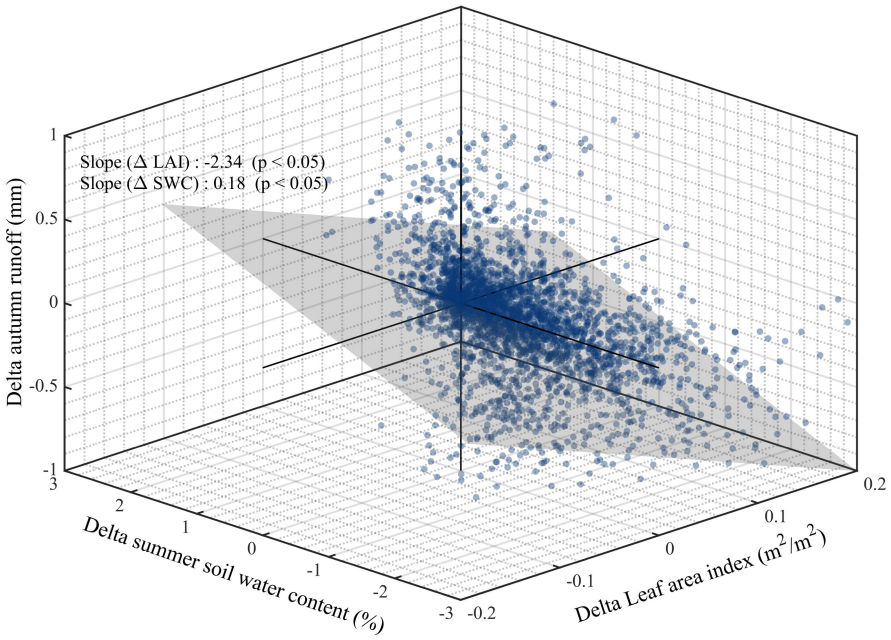

Extended Data Figure 20. The framework diagram of the scenario experiment setting for the LPJ-GUESS model.